Research Article

Nanocoatings of Bovine Serum Albumin on Glass: Effects of pH and Temperature

Sergio-Miguel Acuña-Nelson [iD],[1] **José-Miguel Bastías-Montes,**[1] **Fabiola-Rossana Cerda-Leal,**[1] **Julio-Enrique Parra-Flores** [iD],[2] **Juan-Salvador Aguirre-García,**[3] **and Pedro G. Toledo** [iD][4]

[1]*Departamento de Ingeniería en Alimentos, Universidad del Bío-Bío, Chillán 3780000, Chile*
[2]*Departamento de Nutrición y Salud Pública, Universidad del Bío-Bío, Chillán 3780000, Chile*
[3]*Departamento Agroindustria y Enología, Universidad de Chile, Santiago 8320000, Chile*
[4]*Departamento de Ingeniería Química y Laboratorio de Análisis de Superficies (ASIF), Universidad de Concepción, Concepción 4030000, Chile*

Correspondence should be addressed to Sergio-Miguel Acuña-Nelson; sacuna@ubiobio.cl

Protein adsorption is influenced by many factors such as temperature, pH, protein size and structure, or surface energy and roughness, among others. Self-assembled monolayers (SAMs) and the Langmuir-Blodgett (LB) technique are two of the techniques more used to produces ultrathin films of proteins on surfaces. In this work, we established protocols for the preparation of nanocoatings of bovine serum albumin (BSA) protein on glass surface using SAMs and LB. Furthermore, we determined how small changes in temperature and pH can affect the covering when SAMs are used. Using a combination of different analyses, such as relative roughness, dynamic contact angles, and atomic force microscopy (AFM), it was possible to establish conditions to obtain a uniform nanocoating using SAMs. The results of the analysis of the nanocoating performed using the LB technique were very similar to those obtained using SAMs. The Derjaguin–Landau–Verwey–Overbeek (DLVO) theory in conjunction with the AFM images showed that electrostatic interactions are very important in the self-assembly process, but a process dominated solely by attraction is not sufficient to achieve a good SAM nanocoating, since it does not allow proper orientation and packaging of BSA molecules on the glass surface.

1. Introduction

Adsorption of amphiphilic surfactant molecules at interfaces is a well-known phenomenon of interest in many areas. These adsorption phenomena, jointly with other interactions, have generated many areas of science that interact, and there is great interest in surface modifications that emphasize the development of protocols for the immobilization of nucleic acids, DNA, proteins, lipids, and carbohydrates [1]. At present, protein accumulation and surface modifications have a direct impact in diverse applications in food-processing industries [2], semiconductor materials [3], microbiology [4, 5], biophysics [6–8], biomaterial implants [8–12], biosensors [13–16], nanotechnology [17–19], chromatographic techniques [20–22], filtration membranes [23], and others [24].

In recent years, special attention has been paid to the adsorption of proteins in molecular layers, since under controlled conditions, it is possible to obtain surfaces with new properties, such as offering protection against chemical corrosion or improvement in the biocompatibility of the surface, among others [8–16]. Another way to obtain functional coatings is to use self-assembled multilayer proteins, which are obtained by the successive construction of layers of proteins on top of each other; Aurélien et al. [25] have an interesting review about it. Proteins are the organic molecules found most abundantly in living systems. They show amphiphilic behavior, due to the presence of a mix of polar and nonpolar

groups in their surface, allowing them to act as enzymes, antibodies, antibiotics, hormones, transport molecules, and structural components.

Protein adsorption is influenced by many factors. These factors can be external parameters, such as temperature, pH, ionic strength and buffer composition, or be specific to the protein, such as size, net charge and structure, or to the surface used, such as surface energy, polarity, charge, morphology, and roughness [26–28]. Likewise, the protein adsorption process can be performed over several time scales, from a few seconds to several hours, and may involve electrostatic, hydrophobic, and hydrogen-bonding interactions, and the ability to form π-π stacking [29–35].

The adsorption or the generation of a coating of protein or other organic substance requires that the quantity, arrangement, and conformation of it on the surface be homogeneous, since this will determine the final quality of the coating [26]. However, the preparation of surfaces to be coated with protein in a well-defined molecular arrangement is not trivial. Proteins have much more limited thermal and mechanical stabilities than those of inorganic compounds, so that traditional methods of cutting, polishing, and cleaning in high-vacuum conditions, which are commonly used to obtain coatings of metals and their oxides, are not viable in the case of organic materials. The technique to use to achieve a coating will depend on the type of material and substance to be deposited. In this sense, the most widely used techniques are the self-assembled monolayers (SAMs) and the Langmuir-Blodgett (LB) technique.

SAMs are nanosized coatings that offer a flexible method of carrying out the surface modification of materials to tailor their surface properties for specific end applications [36]. SAMs have their origins in 1946 with the report by Zisman [37] and have been developed in recent years by investigations by Nuzzo and Allara [38]. The technique is based on the adsorption of an active compound onto a substrate as a result of surface chemical reaction (chemisorption), resulting in an organic monolayer of well-defined orientation and packing. So, we can understand self-assembly as the process by which a system moves from a state of disorder towards a state of order, without any external influence [39].

On the other hand, the LB technique produces ultrathin films of amphiphilic molecules having affinity to a liquid surface, such as water, with a hydrophilic group attracted to the solution and the hydrophobic group projecting out of the solution [40]. Depositing of molecules occurs in a controlled manner and the amount of deposited material is known [41].

Although the reasons for using SAMs are several, such as relative easy preparation, no requirement for specialized equipment or special conditions, the ability to be used as building blocks to form other complex structures, or to be the bridge between molecular level nanostructure and macroscopic properties such as wetting or adhesion [42, 43], finding the optimal conditions to manifest these advantages is not simple, and small variations of these optimal conditions can produce large variations in the coatings. In this paper, we use glass as surface, and the protein bovine serum albumin (BSA), a globular protein [44], to compare the two techniques mentioned, SAMs and LB. Furthermore, we try to find the best conditions for both techniques under the studied conditions, and determine, with the help of the classical DLVO theory, how small changes can affect the coatings obtained by SAMs.

2. Materials and Methods

2.1. SAMs.
Glass surfaces (B&C, Germany) washed with ethanol (J.T. Baker) and rinsed with deionized water (EASYpure LF, 18.3 MΩ-cm) were used as the flat substrates. BSA protein (lyophilized powder ≥96%, mol weight ~66 kDa, Sigma-Aldrich) was prepared by dissolving 1 mg/ml in 0.01 M NaCl solution adjusted to three different pH values (4.5, 5.0, and 5.5). These pH values were chosen, because they are close to the isoelectric point, or zero charge point, of the BSA protein [45, 46]. It should be made clear that, under the isoelectric pH, the protein has a positive net charge and on it has a negative net charge. Likewise, the glass surface has a negative surface charge at pH >3 [47]. The flat substrates were submerged in 0.01 M NaCl solution adjusted to the three different pH values for 2, 3, and 4 h at temperatures of 20, 25, and 30°C. After the elapsed time, the substrates were removed and placed in a desiccator until use.

2.2. LB Monolayer.
BSA (0.01 g) was dissolved in 10 ml of deionized water adjusted to pH 5.0. To improve the spreading process, and according to Dervichian [48] and previous work by Sanchez-Gonzalez et al. [49, 50], 100 μl of 1-pentanol ($\rho = 0.890$ g/ml, Merck) was added. Film deposition at the air/water interface was carried out using a microsyringe; 50 μl of solution was deposited on the interface of a Langmuir Balance (KSV 3000), and a time of 10 minutes was considered sufficient to evaporate the amyl alcohol and to equilibrate the protein before compression. As is known, the main parameter that controls the transfer process is the transfer surface pressure, π (mN/m). This value determines the structure and stability of the transferred layer and must be constant during the transfer process. We determined the π value of the subphase for optimal covering.

2.3. Topographic Characterization of Substrates.
Clean and coated substrates were characterized topographically. Commercially available silicon nitride AFM probes were used with nominal square-pyramid tip radius of curvature of 20nm (Veeco). The scan rate was chosen at 2 Hz at the beginning. Spring constants of individual cantilevers were typically 0.2 N/m. Topographic maps of the substrates were obtained using atomic force microscopy (AFM) (Dimension 3100, Digital Instruments) in contact mode for the uncoated substrates and tapping mode for the coated substrates to prevent erosion of the coating. Scans were made at various magnifications (20×20, 10×10, 5×5, and $2 \times 2 \mu$m2) to obtain images and the topographical features observed. Root mean square roughness ($rms = \left(L^{-1} \int_0^L z(x)dx\right)^{1/2}$) was used as a roughness indicator. The Digital Instruments Nanoscope IIIa v4.42 software was used for data acquisition, and the Gwyddion v2.48 software was used for image analysis. To have a more representative area size, the analyzes were performed on the $2 \times 2 \mu$m2 images.

2.4. Dynamic Contact Angle Measurements. Dynamic contact angle was measured using a tensiometer (Sigma 700, KSV). Samples of coated glass with BSA deposited for 2, 3, and 4 hours, and different pHs were immersed in the water-filled tensiometer cup to determine the advancing (immersion) and receding (ascension) dynamic contact angle according to the Wilhelmy method [51]. Data obtained were processed by the software of the equipment (One Attension, v1.7, Biolin Scientific Oy).

2.5. DLVO Theory. Interactions between two colloidal particles can be represented by the total energy of interaction. According to classical DLVO theory, the pressure between two surfaces, such as glass or BSA, in aqueous solution is due to an electric double-layer force, which is almost always repulsive, and a London-van der Waals force, which is almost always attractive. The total energy of interaction between the surfaces at a certain separation distance is obtained by a simple integration of the pressure over the interaction range of interest. Thus,

$$V(L) = V_{vdW}(L) + V_{edl}(L) \tag{1}$$

describes the classical DLVO theory, where V_{vdW} is the London-van der Waals interaction potential, V_{edl} is the electric double layer interaction potential, and L is the distance between surfaces. In Eq. (1), for a sphere (BSA) near a flat surface (glass):

$$V_{vdW}(L) = -\frac{AR}{6L} \tag{2}$$

where A is the nonretarded Hamaker constant (J) and R is the radius of the sphere.

The value of V_{edl} was calculated using the algorithm of McCormack et al. [52] developed to a one-dimensional non-linear Poisson-Boltzmann equation for the mean electrostatic potential, $\psi(L)$, in a symmetric $v:v$ electrolyte between two planar surfaces located at a distance L apart, which can be written in the nondimensional form:

$$\frac{d^2 y(\xi)}{d\xi^2} = \sinh y(\xi) \tag{3}$$

where $y = (ev\psi/kBT)$ is the potential scaled by the thermal potential (kBT/ev), with e being the protonic charge, kB the Boltzmann constant, and T the absolute temperature. L is related to the scaled variable $\xi = \kappa L$ by the Debye length $\kappa - 1 = (8\pi n v^2 e^2/\epsilon kBT) - 1/2$, where ϵ is the dielectric constant of the solvent and n is the number of ions in the bulk electrolyte.

For calculation purposes, the BSA molecule was assumed to be a sphere with radius $R = 3.9$ nm [53]. The Hamaker constant was obtained using combinations relations (or combining laws) [54], which are used to obtain approximate values for unknown Hamaker constants in terms of known ones. For this, we define $Aswp$ as the nonretarded Hamaker constant for silica (s) and BSA (p) interacting across water

TABLE 1: Dynamic contact angles of water (in degrees), hysteresis, and mean roughness of a clean glass ($N = 5$).

θ advancing	θ receding	Hysteresis*	RMS (nm)
51.3 ± 1.9	46.6 ± 1.5	0.06 ± 0.01	0.79 ± 0.09

*Hysteresis: $|cos\theta advancing - cos\theta receding|$.

(w), and we may expect that $Aswp$ to be approximately related to $Asws$ and $Apwp$ via

$$A_{swp} \approx \pm \sqrt{A_{sws} A_{pwp}} \tag{4}$$

using the values of $Asws = 4.114 \times 10 - 21$ J [55] and $Apwp = 4.6 \times 10 - 21$ J [56].

3. Results and Discussion

Table 1 shows the values of dynamic contact angles obtained for clean glass. The measurements made with deionized water include the advancing and receding contact angles and the hysteresis of the system. The results reflect the affinity between clean glass and water, which is due to the silanol, SiOH groups on the surface of the glass, which form hydrogen bonds with water molecules. The low hysteresis value, 0.06, indicates that the surface of the glass is relatively smooth.

Figure 1 shows AFM images of a clean glass surface, in which a relatively smooth surface is observed, with very few imperfections and some typical surface granules, which agrees with the roughness analysis, which showed a low average roughness of 0.79 nm.

The dynamic contact angles measured for the coated substrates; Table 2 shows an increase in the hydrophobicity of the substrate with respect to the uncoated substrate (Table 1), which shows that the protein molecule is adsorbed on the glass through its hydrophilic part, projecting its hydrophobic part outwards. It is believed that increasing the temperature generates a greater driving force for adsorption, which would be due to an entropy gain derived from the release of water molecules and salt ions adsorbed on the surface and structural rearrangements within the protein [26]. Our results shown in Table 2 indicate that, as the temperature changes, the orientation of the molecules on the glass surface also changes, at the three pH levels studied, since the highest values of contact angle were obtained at a temperature of 20°C, while the lowest values were obtained at 25°C. We believe that above is due to the fact that not all proteins behave in the same way, and this can be observed in Table 2, where it can be seen that at the three pH levels studied, there is a decrease in the measured contact angles when increasing the temperature from 20 to 25°C, but when the temperature is increased again, to 30°C, the measured contact angles increase; that is, the temperature has effects on the equilibrium state of the BSA protein that affect the orientation adopted by the protein when it is deposited on the glass surface. Our results show that at temperatures of 20 and 30°C, the BSA protein prefers to interact with itself rather
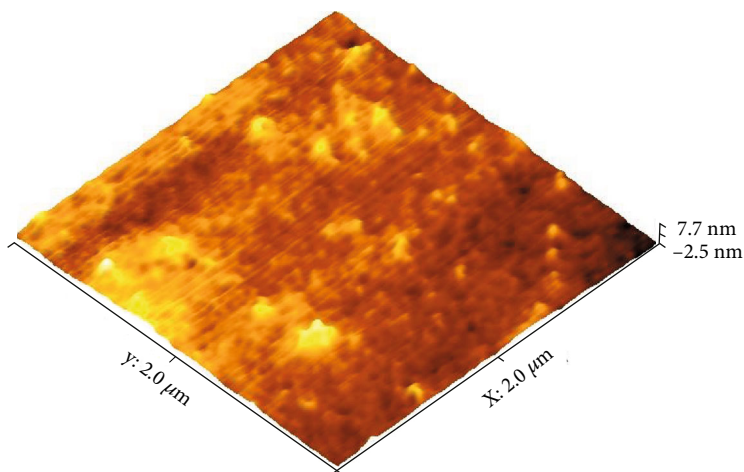
FIGURE 1: AFM images of a flat glass substrate washed with ethanol and used for coatings with BSA, scan of $2 \times 2\ \mu$m2.

TABLE 2: Dynamic contact angles (degrees) of water on BSA protein SAMs on glass prepared under different conditions of temperatures and pH ($N = 5$).

pH	Temperature		Immersion time		
			2 h	3 h	4 h
4.5	20°C	Advancing contact angle (°)	94.9 ± 5.3	80.6 ± 5.1	79.9 ± 4.8
		Receding contact angle (°)	56.5 ± 3.2	58.9 ± 3.9	57.2 ± 4.1
		Hysteresis	0.63 ± 0.11	0.35 ± 0.13	0.36 ± 0.12
	25°C	Advancing contact angle (°)	79.9 ± 4.1	82.3 ± 3.9	83.2 ± 4.6
		Receding contact angle (°)	36.0 ± 3.3	36.4 ± 2.9	36.6 ± 3.7
		Hysteresis	0.63 ± 0.10	0.67 ± 0.14	0.68 ± 0.13
	30°C	Advancing contact angle (°)	90.4 ± 5.4	89.2 ± 5.1	83.4 ± 5.2
		Receding contact angle (°)	52.2 ± 4.3	54.5 ± 3.8	56.0 ± 3.7
		Hysteresis	0.61 ± 0.13	0.54 ± 0.10	0.44 ± 0.11
5.0	20°C	Advancing contact angle (°)	76.6 ± 4.1	78.3 ± 3.6	75.5 ± 4.6
		Receding contact angle (°)	58.6 ± 4.8	60.4 ± 3.9	58.4 ± 4.2
		Hysteresis	0.28 ± 0.06	0.29 ± 0.05	0.27 ± 0.06
	25°C	Advancing contact angle (°)	71.7 ± 3.8	71.0 ± 3.9	68.8 ± 2.9
		Receding contact angle (°)	37.4 ± 3.2	40.3 ± 3.6	45.9 ± 3.1
		Hysteresis	0.48 ± 0.09	0.43 ± 0.09	0.33 ± 0.07
	30°C	Advancing contact angle (°)	87.1 ± 4.2	88.7 ± 3.9	84.8 ± 3.8
		Receding contact angle (°)	58.6 ± 3.6	60.4 ± 3.1	58.4 ± 3.0
		Hysteresis	0.47 ± 0.10	0.47 ± 0.08	0.43 ± 0.08
5.5	20°C	Advancing contact angle (°)	89.0 ± 5.5	83.4 ± 5.1	74.2 ± 4.8
		Receding contact angle (°)	82.6 ± 4.4	75.6 ± 4.3	71.3 ± 4.2
		Hysteresis	0.55 ± 0.11	0.38 ± 0.09	0.27 ± 0.06
	25°C	Advancing contact angle (°)	82.6 ± 5.0	75.6 ± 3.7	71.3 ± 3.8
		Receding contact angle (°)	40.9 ± 3.3	39.9 ± 3.5	46.5 ± 3.8
		Hysteresis	0.62 ± 0.12	0.51 ± 0.11	0.36 ± 0.07
	30°C	Advancing contact angle (°)	83.9 ± 4.4	79.4 ± 4.1	82.8 ± 4.5
		Receding contact angle (°)	55.2 ± 3.1	57.7 ± 3.2	60.4 ± 3.2
		Hysteresis	0.46 ± 0.10	0.35 ± 0.07	0.36 ± 0.07

TABLE 3: Relative roughness (RMS) and average height of BSA protein SAMs on glass prepared under different temperatures and pH levels.

| pH | Temperature | | Immersion time | | |
			2 h	3 h	4 h
4.5	20°C	RMS (nm)	5.59 ± 0.15	4.12 ± 0.12	6.11 ± 0.14
		Average height (nm)	7.04 ± 0.20	10.28 ± 0.31	12.52 ± 0.28
	25°C	RMS (nm)	3.26 ± 0.13	1.66 ± 0.36	1.41 ± 0.25
		Average height (nm)	10.82 ± 0.41	6.35 ± 0.32	5.40 ± 0.23
	30°C	RMS (nm)	1.39 ± 0.37	1.20 ± 0.35	1.03 ± 0.19
		Average height (nm)	11.38 ± 0.28	12.93 ± 0.24	13.24 ± 0.31
5.0	20°C	RMS (nm)	4.46 ± 0.18	1.83 ± 0.37	7.78 ± 0.35
		Average height (nm)	7.37 ± 0.36	5.61 ± 0.30	3.01 ± 0.15
	25°C	RMS (nm)	1.32 ± 0.17	0.71 ± 0.15	0.39 ± 0.09
		Average height (nm)	4.14 ± 0.21	2.20 ± 0.20	1.84 ± 0.16
	30°C	RMS (nm)	20.97 ± 0.93	7.89 ± 0.48	15.22 ± 0.44
		Average height (nm)	25.03 ± 0.97	8.57 ± 0.42	18.62 ± 0.21
5.5	20°C	RMS (nm)	0.97 ± 0.18	0.47 ± 0.10	2.72 ± 0.27
		Average height (nm)	10.36 ± 0.33	13.11 ± 0.32	13.47 ± 0.29
	25°C	RMS (nm)	1.19 ± 0.21	0.38 ± 0.11	1.26 ± 0.25
		Average height (nm)	6.81 ± 0.34	12.74 ± 0.31	12.79 ± 0.49
	30°C	RMS (nm)	0.43 ± 0.12	4.55 ± 0.38	0.54 ± 0.14
		Average height (nm)	11.74 ± 0.26	13.29 ± 0.37	11.79 ± 0.23

than with the surface, allowing BSA orientations that favor the formation of aggregates or clusters of the protein.

When observing the topographic results obtained for the conditions studied, we can see that the temperature not only affected the orientation of the BSA on the glass but also affected the amount of protein adsorbed. The topographic characterization allowed the appreciation that, when working at temperatures of 20 and 30°C, irregularly coated glass surfaces were obtained, with BSA protein clusters and the presence of large peaks on all the surfaces analyzed. Table 3 shows the roughness analysis of the samples studied, where it is possible to appreciate that at temperatures of 20 and 30°C, the greatest relative roughness and the highest average height were observed. The values of roughness and average height, obtained at 20 and 30°C allow us to infer that the samples at these temperatures have coatings with greater imperfections than those observed at 25°C. AFM images of the samples obtained at 20 and 30°C are presented in supporting information S1. The advancing contact angle of 68.8° for water on the BSA protein-coated glass surface at pH 5.0 and 25°C after 4 h of immersion is similar to the values previously reported [7, 50, 57]. Follstaedt et al. [57] obtained similar values for contact angles on an Octadecyltrimethoxysilane (OTMS)-coated surface and obtained values for contact angles similar to ours and the relative roughness of 2.7 nm, which in our case fluctuates depending on conditions. The same authors establish that these differences may be due to the fact that the asymmetric shape of the BSA protein does not allow the protein to always be oriented in the same way on the surface.

Regarding the coating formed at pH 5.0 and 25°C, the images show coatings more homogeneous coatings than those form under the other conditions studied. In addition, as the time of immersion increases, the coatings become softer and contain fewer imperfections, as shown in Table 3. At pH levels of 4.5 and pH 5.5, the behavior observed was similar to that described above, i.e., large protein clusters and uneven surfaces (see Supplementary Material S1).

Figure 2 shows AFM images of the glass surface coated with BSA at pH 5.0, a temperature of 25°C and 4 h of immersion. A smooth surface can be observed, with no superficial imperfections, and the surface is highly homogeneous. The height profile (Figure 3(c)) reveals that the BSA coating does not show great variations in height, displaying, in general, a flat profile. Likewise, the relative roughness value obtained for this coating, 0.39 nm, as well as its average height, 1.84 nm, were the lowest of all the samples studied (see Table 3).

Our results indicate that the charge distribution on the BSA protein is governed by the pH of the medium which also controls the degree of adsorption of BSA on the glass surface. It has been determined that the isoelectric point (IP), or point of zero charge, of BSA is close to pH 4.8 [45, 46]; therefore, at higher pH levels, negative charges will be generated; at lower pH levels, positive charges will be generated. On the other hand, the surface potential of the glass is negative in the range of pH and NaCl concentration studied [47]. According to the above, higher adsorption was expected at pH 4.5 because the electrostatic interactions would favor it, but this did not occur. At pH 4.5, the
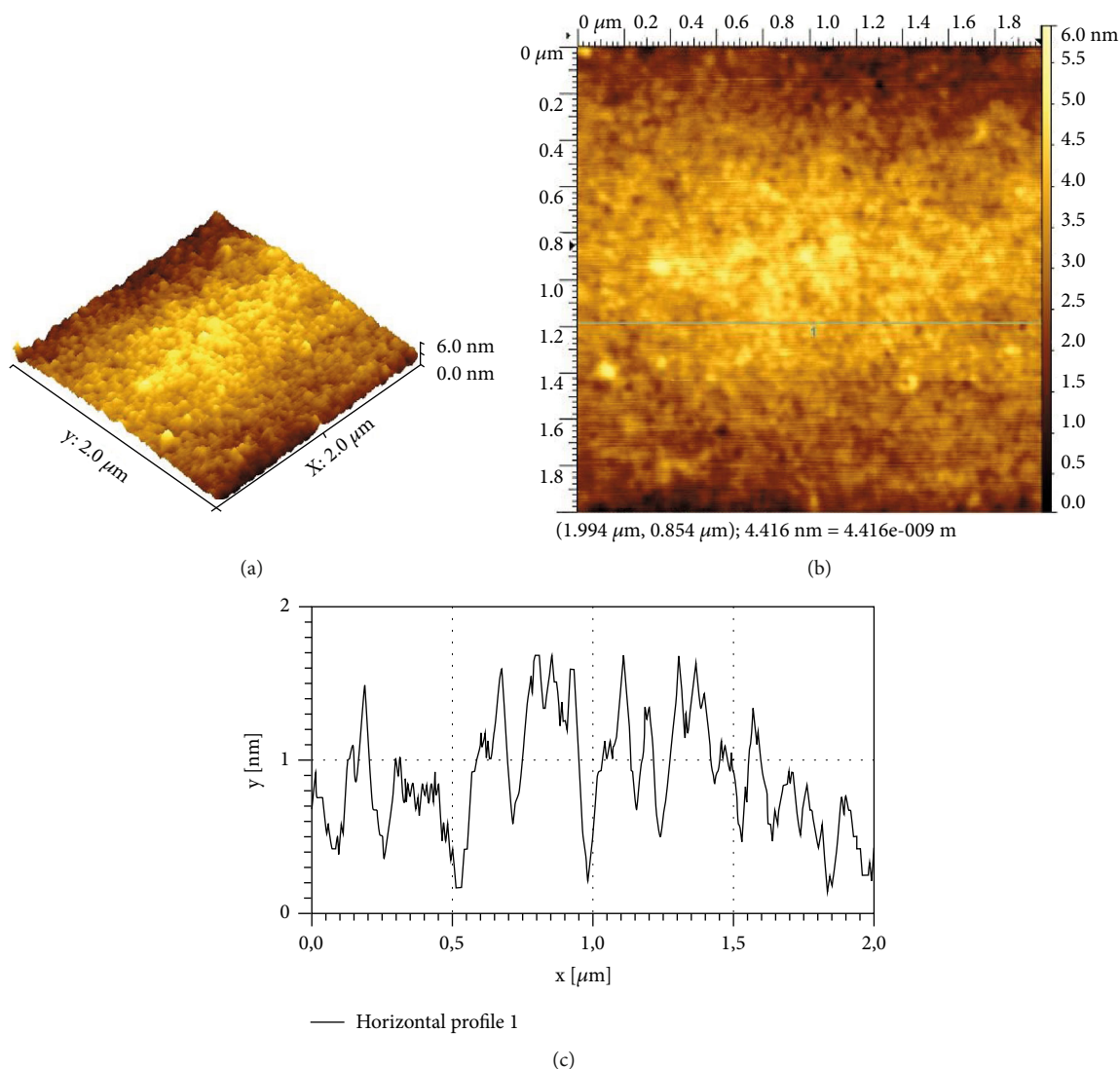
(a)

(1.994 μm, 0.854 μm); 4.416 nm = 4.416e-009 m

(b)

—— Horizontal profile 1

(c)

FIGURE 2: AFM image of BSA protein SAMs on glass prepared at pH 5.0, 25°C, and 4 h immersion: (a) 3D image, scan of $2 \times 2 \, \mu m$; (b) 2D image, green line indicates the cut profile; (c) height profile cut of image.

coating was not homogeneous, showing protein clusters on the glass surface.

The continuum DLVO theory has been used to describe the surface interaction down to a separation of 1-2 nm. In this theory, only the repulsive electric double-layer force and the attractive van der Waals force matter, since they operate at long range, over 1-2 nm. Here, repulsive double-layer interactions in the BSA protein-glass system were calculated by solving the nonlinear Poisson-Boltzmann equation with the algorithm proposed by McCormack et al. [52], using 51.3 mV as the surface potential value of glass [57], for the three pH levels studied, while for the BSA the following surface potential values were used: 4 mV at pH = 4.5, -7 mV at pH = 5.0, and -12 mV at pH = 5.5 [53]. On the other hand, for the calculation of nonretarded van der Waals attractions, for the same system, we used a Hamaker constant value of $Aswp = 4.35 \times 10 - 21$ J in equation (4). Figure 3 shows the interaction curves for the protein-glass system at the three pH levels studied, in which three different behaviors can be

observed, depending on the surface potentials of the surfaces. At pH 4.5, when the protein has positive surface potential, the interaction is clearly attractive. The above could be beneficial, but as our images showed, that was not the case. Apparently, an excess of attraction produces protein clusters, disfavoring a uniform coating. The presence of a higher density of positive charges induces lateral repulsions between the protein molecules, which is detrimental to a good adsorption of BSA on the glass surface. On the other hand, when the pH is significantly above the IP, as in our case at pH 5.5, where the glass surface and the protein have negative surface potential of -12 mV, the interaction with glass surface is repulsive until the separation distances closest to 3 nm, the distance at which the van der Waals forces begin to manifest themselves and the interaction becomes attractive. Obviously, an excess of charge, negative in this case, will produce a greater repulsion between the BSA protein molecules, due to lateral interactions, and with the glass surface, also negatively charge, which will result in a poor coating, as observed in
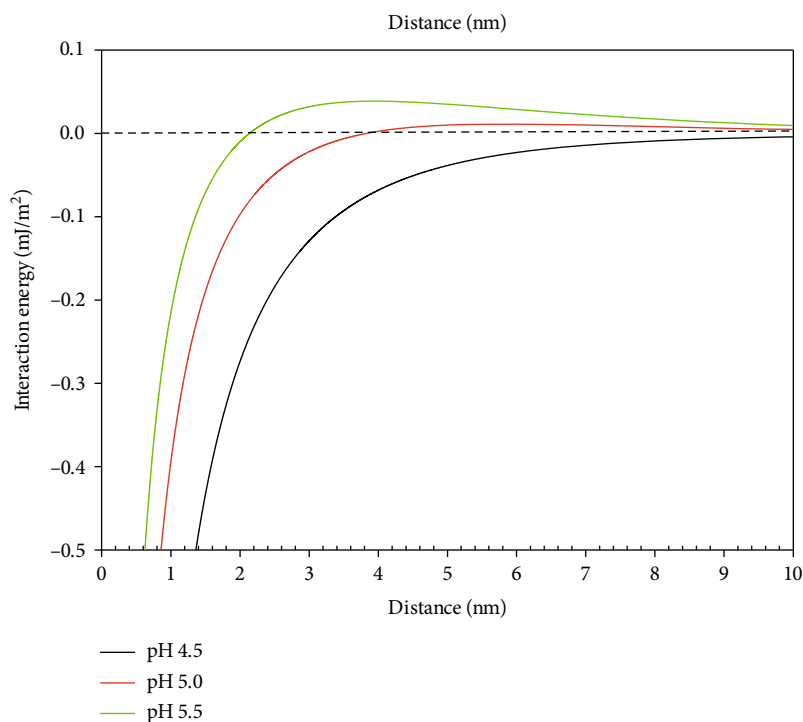
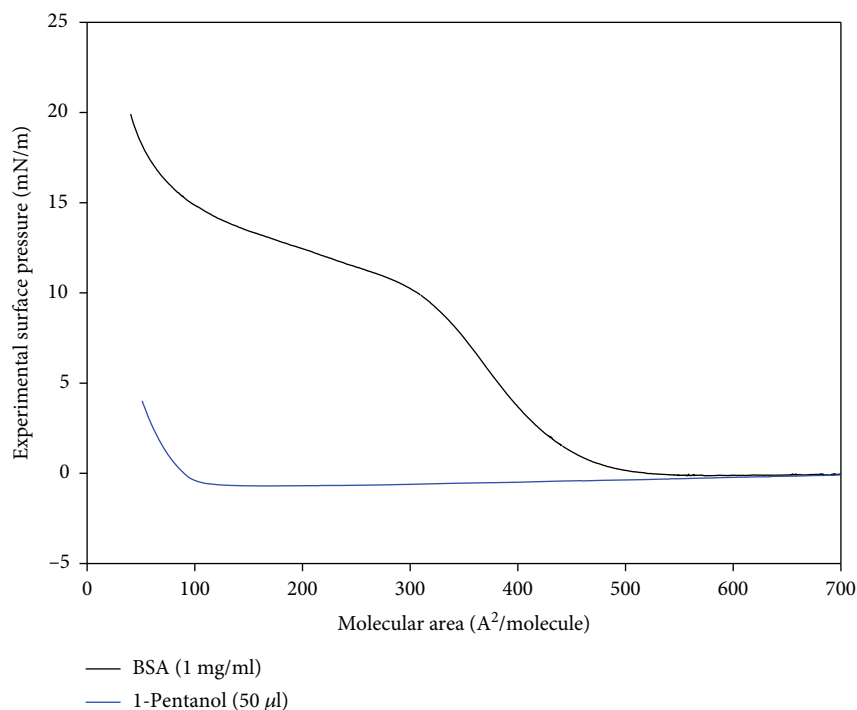Figure 3: DLVO curves between BSA protein and a glass surface in 0.01 M NaCl.

Figure 4: Comparison between pressure isotherm of BSA (black line) and 1-pentanol (blue line).

the images (S1). At pH 5.0, when the BSA protein has a slightly negative surface potential of -7 mV and the interaction is repulsive, this only happens until the separation distances closest to 6-7 nm; at this distance, the van der Waals attractive forces begin to manifest themselves, and adsorption of BSA on the glass occurs. The aforementioned distance, 6-7 nm, is very close to the diameter of a BSA protein molecule, 7.8 nm [53]. Apparently, this allows the BSA molecules to adsorb better on the glass surface by allowing the protein molecules to be oriented and packed in a more compact way on the glass surface. According to Rabe et al. [26], because proteins have a complex structure, they exhibit

(a)

(1.357 um, 0.002 um); 0.923 nm = 9.231e-010 m
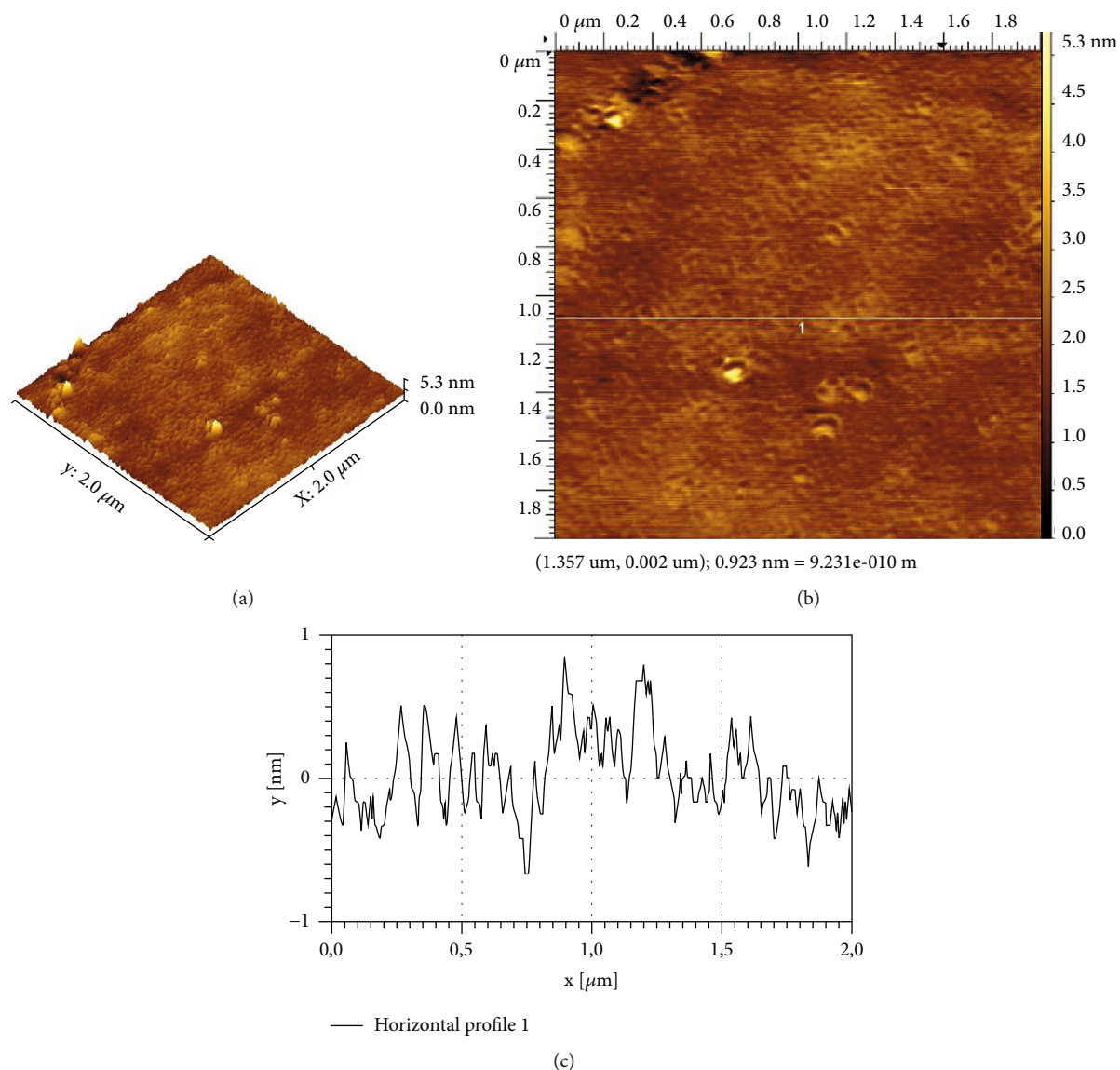
(b)

— Horizontal profile 1

(c)

FIGURE 5: AFM images of a glass surface coated with BSA using the LB technique at a surface pressure of 6 mN/m and pH 5.0: (a) 3D image, scan of $2 \times 2 \, \mu$m2; (b) 2D image, green line indicates the cut profile; (c) high-profile cut of image.

different affinities in different regions of their surface, which will depend, mainly, on the local composition of the amino acid residues. Thus, the orientation adopted by the protein BSA on the glass surface will tend to reduce its free energy, which will be, among others, the result of attractive interactions, hydrogen bonds, and the increase in entropy due to the release of counterions and solvent molecules.

Our results show that at pH 5.0, 25°C, and 4 h immersion, the BSA protein has the best orientation and conditions to adsorb on the glass surface, allowing it to lose energy by reducing the attractive forces towards the surface and, at the same time, gain free energy because the repulsive forces between neighboring proteins reduce.

Figures 4 and 5 show the results obtained when coating a glass surface with BSA using the LB technique. Achieving the coating of BSA protein on the glass surface by the LB technique requires two successive processes: the first is the adsorption of BSA protein at the air-water interface, and the second is its transfer and immobilization on the surface of the glass. For Pal et al. [58], these two stages are key when using the LB technique and define the efficiency of the coating and its quality. Figure 4 shows the ability of 1-pentanol to carry the BSA protein to the air-water interface. It compares the surface pressure of pure 1-pentanol and 1-pentanol with BSA after 10 minutes of deposition on water. The difference in the surface pressure curves obtained is evident; after 10 minutes, the curve of pure 1-pentanol shows that no 1-pentanol remains on the surface of the water. Thus, the curve obtained for the 1-pentanol-BSA mixture is actually due only to the presence of BSA at the air-water interface. The transfer of molecular monolayers from the air-water interface to the substrate using the LB technique must be carried out by maintaining the system at a constant pressure. Ideally, this pressure should be within the area of the

TABLE 4: Dynamic contact angles of water (°), hysteresis, and mean roughness of a glass surface coated with BSA using the LB technique ($N = 5$).

θ advancing	θ receding	Hysteresis*	RMS (nm)
75.1 ± 2.9	57.4 ± 4.3	0.61 ± 0.10	0.35 ± 0.04

*Hysteresis: $|cos\theta \text{advancing} - cos\theta \text{receding}|$.

isotherm of the BSA curve (see Figure 4), where its behavior satisfies the condensed liquid state. Therefore, coating the glass surface with BSA using the LB technique were made at a surface pressure of 6 mN/m.

Table 4 shows the results obtained for the glass surface coated with BSA using the LB technique at a surface pressure of 6 mN/m. The average value of advancing contact angle obtained, 75.1°, is very close to that obtained by SAMs at pH 5.0, 25°C, and 4 h immersion (68.8°) and that reported by Sánchez-González et al. [49], who obtained a contact angle value of 73° using the same technique.

Figures 5(a) and 5(b) show $2 \times 2 \mu$m2 AFM images of a glass surface coated with BSA, where a homogeneous surface is observed. The roughness analysis of the samples gave low values of average roughness, 0.34 nm, as shown in Table 4. The height profile (Figure 5(c)) reveals that the coating did not show a large variation in the height of the samples, which confirms that the coating was smooth and homogeneous.

4. Conclusions

Nanocoatings of BSA protein on glass surface, produced using self-assembled monolayer (SAM) and Langmuir-Blodgett (LB) techniques, show that the preparation of these coatings is reproducible by following the procedures described. Through a combination of different analyzes, such as relative roughness, dynamic contact angles, and AFM images, it was possible to establish conditions to obtain a uniform nanocoating with SAM, pH of 5.0, a temperature of 25°C, and an immersion time of 4 h. Our results also show that small changes in temperature or pH that can affect the coatings, since these changes will affect the orientation adopted by the BSA protein on the glass surface, which tends to reduce its free energy, but that due to these changes, it will affect its attractive interactions, hydrogen bonds, and entropy due to the release of counterions and solvent molecules. The results of the analysis of the nanocoating performed using the LB technique were very similar to those obtained using SAM. The DLVO theory in conjunction with the AFM images showed that electrostatic interactions are very important in the self-assembly process, but that a process dominated by attraction alone is not sufficient for achieving a nanocoating using SAM, since it does not allow adequate orientation and packing of the BSA molecules on the glass surface.

Data Availability

Data is stored in a cloud, if required, please send an email to: sacuna@ubiobio.cl

Conflicts of Interest

The authors declare that there is no conflict of interest regarding the publication of this paper.

Supplementary Materials

S1 AFM images of the samples obtained at 20, 25, and 30°C. (*Supplementary Materials*)

References

[1] R. S. Matson, *Microarray Methods and Protocols*, CRC Press, Boca Raton, 2009.

[2] S. Zouaghi, T. Six, S. Bellayer et al., "Antifouling biomimetic liquid-infused stainless steel: application to dairy industrial processing," *ACS Applied Materials & Interfaces*, vol. 9, no. 31, pp. 26565–26573, 2017.

[3] R. K. Gupta and R. A. Singh, "Preparation and characterization of electrically conducting Langmuir–Blodgett films of poly(N-octadecylaniline)," *Journal of Colloid and Interface Science*, vol. 285, no. 1, pp. 67–73, 2005.

[4] J. W. Costerton, K. J. Cheng, G. G. Geesey et al., "Bacterial biofilms in nature and disease," *Annual Review of Microbiology*, vol. 41, no. 1, pp. 435–464, 1987.

[5] K. Ijiro, Y. Matsuo, and M. Shimomura, "Stretching of single DNA molecules by LB technique for restriction site mapping," *Nucleic Acids Symposium Series*, vol. 3, no. 1, pp. 47-48, 2003.

[6] S. A. Vickery and R. C. Dunn, "Scanning near-field fluorescence resonance energy transfer microscopy," *Biophysical Journal*, vol. 76, no. 4, pp. 1812–1818, 1999.

[7] Y. L. Jeyachandran, J. A. Mielczarski, E. Mielczarski, and B. Rai, "Efficiency of blocking of non-specific interaction of different proteins by BSA adsorbed on hydrophobic and hydrophilic surfaces," *Journal of Colloid and Interface Science*, vol. 341, no. 1, pp. 136–142, 2010.

[8] S. M. Acuña, J. M. Bastías, and P. G. Toledo, "Direct measurement of interaction forces between bovine serum albumin and poly(ethylene oxide) in water and electrolyte solutions," *Plos One*, vol. 12, no. 3, p. e0173910, 2017.

[9] L. Vroman and A. L. Adams, "Adsorption of proteins out of plasma and solutions in narrow spaces," *Journal of Colloid and Interface Science*, vol. 111, no. 2, pp. 391–402, 1986.

[10] S. J. McClellan and E. I. Franses, "Adsorption of bovine serum albumin at solid/aqueous interfaces," *Colloids and Surfaces A: Physicochemical and Engineering Aspects*, vol. 260, no. 1-3, pp. 265–275, 2005.

[11] M. Rankl, T. Ruckstuhl, M. Rabe, G. R. J. Artus, A. Walser, and S. Seeger, "Conformational reorientation of immunoglobulin G during nonspecific interaction with surfaces," *ChemPhysChem*, vol. 7, no. 4, pp. 837–846, 2006.

[12] X. Wang, J. Miao, H. Zhao, C. Mao, X. Chen, and J. Shen, "Fabrication of nonbiofouling metal stent and in vitro studies on its hemocompatibility," *Journal of Biomaterials Applications*, vol. 29, pp. 14–25, 2013.

[13] M. P. Byfield and R. A. Abuknesha, "Biochemical aspects of biosensors," *Biosensors & Bioelectronics*, vol. 9, no. 4-5, pp. 373–399, 1994.

[14] N. K. Chaki and K. Vijayamohanan, "Self-assembled monolayers as a tunable platform for biosensor applications," *Biosensors & Bioelectronics*, vol. 17, no. 1-2, pp. 1–12, 2002.

[15] F. Davis and S. P. J. Higson, "Structured thin films as functional components within biosensors," *Biosensors & Bioelectronics*, vol. 21, no. 1, pp. 1–20, 2005.

[16] S. A. Bhakta, E. Evans, T. E. Benavidez, and C. D. Garcia, "Protein adsorption onto nanomaterials for the development of biosensors and analytical devices: a review," *Analytica Chimia Acta*, vol. 872, pp. 7–25, 2015.

[17] E. Mouri, K. Matsumoto, and H. Matsuoka, "Effect of pH on the nanostructure of an amphiphilic carbosilane/methacrylic acid block copolymer at air/water interface," *Journal of Applied Crystallography*, vol. 36, no. 3, pp. 722–726, 2003.

[18] T. Y. Liu, S. Y. Chen, D. M. Liu, and S. C. Liou, "On the study of BSA-loaded calcium-deficient hydroxyapatite nano-carriers for controlled drug delivery," *Journal of Controlled Release*, vol. 107, no. 1, pp. 112–121, 2005.

[19] A. Ravindran, A. Singh, A. M. Raichur, N. Chandrasekaran, and A. Mukherjee, "Studies on interaction of colloidal Ag nanoparticles with bovine serum albumin (BSA)," *Colloids and Surfaces B: Biointerfaces*, vol. 76, no. 1, pp. 32–37, 2010.

[20] A. S. Freed and S. M. Cramer, "Protein–Surface interaction maps for ion-exchange chromatography," *Langmuir*, vol. 27, no. 7, pp. 3561–3568, 2011.

[21] F. Dismer and J. Hubbuch, "3D structure-based protein retention prediction for ion-exchange chromatography," *Journal of Chromatography A*, vol. 1217, no. 8, pp. 1343–1353, 2010.

[22] L. Yu, L. Zhang, and Y. Sun, "Protein behavior at surfaces: orientation, conformational transitions and transport," *Journal of Chromatography A*, vol. 1382, pp. 118–134, 2015.

[23] L. D. Tijing, Y. C. Woo, J. S. Choi, S. Lee, S. H. Kim, and H. K. Shon, "Fouling and its control in membrane distillation–A review," *Journal of Membrane Science*, vol. 475, pp. 215–244, 2015.

[24] C. McGlothin, C. Rosu, L. Jiang, V. Breedveld, and D. W. Hess, "Lowering protein fouling by rational processing of fluorine-free hydrophobic coatings," *Surface and Interfaces*, vol. 17, p. 100370, 2019.

[25] V. S. Aurélien, L. Damien, D.-C. Sophie, and D.-G. Christine, "Protein-based polyelectrolyte multilayers," *Advances in Colloid and Interface Science*, vol. 280, p. 102161, 2020.

[26] M. Rabe, D. Verdes, and S. Seeger, "Understanding protein adsorption phenomena at solid surfaces," *Advances in Colloid and Interface Science*, vol. 162, no. 1-2, pp. 87–106, 2011.

[27] M. M. Ouberai, K. Xu, and M. E. Welland, "Effect of the interplay between protein and surface on the properties of adsorbed protein layers," *Biomaterials*, vol. 35, no. 24, pp. 6157–6163, 2014.

[28] P. E. Scopelliti, A. Borgonovo, M. Indrieri et al., "The effect of surface nanometre-scale morphology on protein adsorption," *PLoS One*, vol. 5, no. 7, article e11862, 2010.

[29] J. P. Andrade, *Surface and Interfacial Aspects of Biomedical Polymers, Volume 2 Protein Adsorption*, Plenum, New York, 1985.

[30] V. Puddu and C. C. Perry, "Peptide adsorption on silica nanoparticles: evidence of hydrophobic interactions," *ACS Nano*, vol. 6, no. 7, pp. 6356–6363, 2012.

[31] K. Scida, P. W. Stege, G. Haby, G. A. Messina, and C. D. García, "Recent applications of carbon-based nanomaterials in analytical chemistry: critical review," *Analytica Chimica Acta*, vol. 691, no. 1-2, pp. 6–17, 2011.

[32] P. Roach, N. J. Shirtcliffe, D. Farrar, and C. C. Perry, "Quantification of surface-bound proteins by fluorometric assay: comparison with quartz crystal microbalance and amido black assay," *The Journal of Physical Chemistry B*, vol. 110, pp. 20572–20579, 2011.

[33] R. Ishiguro, Y. Yokoyama, H. Maeda, A. Shimamura, K. Kameyama, and K. Hiramatsu, "Modes of conformational changes of proteins adsorbed on a planar hydrophobic polymer surface reflecting their adsorption behaviors," *Journal of Colloid and Interface Science*, vol. 290, no. 1, pp. 91–101, 2005.

[34] K. Kandori, M. Mukai, A. Fujiwara, A. Yasukawa, and T. Ishikawa, "Adsorption of bovine serum albumin and lysozyme on hydrophobic calcium hydroxyapatites," *Journal of Colloid and Interface Science*, vol. 212, no. 2, pp. 600–603, 1999.

[35] C. E. Giacomelli, M. J. Avena, and P. De Pauli, "Adsorption of bovine serum albumin onto TiO_2 Particles," *Journal of Colloid and Interface Science*, vol. 188, no. 2, pp. 387–395, 1997.

[36] A. Mahapatro, "Bio-functional nano-coatings on metallic biomaterials," *Materials Science and Engineering C*, vol. 55, pp. 227–251, 2015.

[37] W. C. Bigelow, D. L. Pickett, and W. A. Zisman, "Oleophobic monolayers: I. Films adsorbed from solution in non-polar liquids," *Journal of Colloid and Interface Science*, vol. 1, no. 6, pp. 513–538, 1946.

[38] R. G. Nuzzo and D. L. Allara, "Adsorption of bifunctional organic disulfides on gold surfaces," *Journal of the American Chemical Society*, vol. 105, no. 13, pp. 4481–4483, 1983.

[39] A. Ulman, "Formation and structure of self-assembled monolayers," *Chemical Reviews*, vol. 96, no. 4, pp. 1533–1554, 1996.

[40] G. L. Gaines Jr., *Insoluble Monolayers at Liquid-Gas Interfaces*, Interscience, New York, 1966.

[41] L. Godínez, "Substratos modificados con monocapas autoensambladas: dispositivos para fabricar sensores y estudiar procesos químicos y fisicoquímicos interfaciales," *Revista de la Sociedad Química de México*, vol. 43, pp. 219–2229, 1999.

[42] J. C. Love, L. A. Estroff, J. K. Kriebel, R. G. Nuzzo, and G. M. Whitsides, "Self-Assembled monolayers of Thiolates on metals as a form of nanotechnology," *Chemical Reviews*, vol. 105, no. 4, pp. 1103–1170, 2005.

[43] F. Schreiber, "Structure and growth of self-assembling monolayers," *Progress in Surface Science*, vol. 65, no. 5-8, pp. 151–257, 2000.

[44] T. Peters Jr. and R. G. Reed, "Serum albumin: conformation and active sites," *Proceedings of FEBS Management*, vol. 50, pp. 11–13, 1977.

[45] J. D. Andrade, V. Hlady, and A. P. Wei, "Adsorption of complex proteins at interfaces," *Pure and Applied Chemistry*, vol. 64, no. 11, pp. 1777–1781, 1992.

[46] W. Li and S. Li, "A study on the adsorption of bovine serum albumin onto electrostatic microspheres: role of surface groups," *Colloids and Surfaces A: Physicochemical and Engineering Aspects*, vol. 295, no. 1-3, pp. 159–164, 2007.

[47] S. M. Acuña and P. G. Toledo, "Short-Range forces between glass surfaces in aqueous solutions," *Langmuir*, vol. 24, no. 9, pp. 4881–4887, 2008.

[48] D. Dervichian, "A New Technique for the Spreading of Proteins and the "Spreading Number"," *Nature*, vol. 144, no. 3649, pp. 629-630, 1939.

[49] J. Sanchez-González, M. A. Cabrerizo-Vilchez, and M. J. Galvez-Ruiz, "Evaluation of the interactions between lipids and γ -globulin protein at the air-liquid interface," *Colloids and Surfaces B*, vol. 12, no. 3-6, pp. 123–138, 1999.

[50] J. Sánchez-González, J. Ruiz, and M. J. Gálvez, "Langmuir-Blodgett films of biopolymers: a method to obtain protein multilayers," *Journal of Colloid and Interface Science*, vol. 267, no. 2, pp. 286–293, 2003.

[51] A. Adamson and A. Gast, *Physical Chemistry of Surfaces*, Wiley, New York, 6th edition, 1997.

[52] D. McCormack, S. L. Carnie, and D. Y. C. Chan, "Calculations of electric double-layer force and interaction free energy between dissimilar surfaces," *Journal of Colloid and Interface Science*, vol. 169, no. 1, pp. 177–196, 1995.

[53] V. Valiño, M. F. San Roman, R. Ibañez, J. M. Benito, I. Escudero, and I. Ortiz, "Accurate determination of key surface properties that determine the efficient separation of bovine milk BSA and LF proteins," *Separation and Purification Technology*, vol. 135, pp. 145–157, 2014.

[54] J. N. Israelachvili, *Intermolecular and Surface Forces*, Academic Press, Amsterdam, 3rd edition, 2011.

[55] S. Ikeda and K. Nishinari, "Intermolecular forces in bovine serum albumin solutions exhibiting Solidlike mechanical behaviors," *Biomacromolecules*, vol. 1, no. 4, pp. 757–763, 2000.

[56] L. Bergström, "Hamaker constants of inorganic materials," *Advances in Colloid Interface Science*, vol. 70, pp. 125–169, 1997.

[57] S. C. Follstaedt, J. A. Last, D. K. Cheung, P. L. Gourley, and D. Y. Sasaki, *Protein adhesion on SAM coated semiconductor wafers: hydrophobic versus hydrophilic surfaces*, Sandia Natl Lab [Tech Rep] SAND, Albuquerque, 2000.

[58] P. Pal, T. Kamilya, M. Mahato, and G. B. Talapatra, "The formation of pepsin monomolecular layer by the Langmuir-Blodgett film deposition technique," *Colloids and Surfaces B: Biointerfaces*, vol. 73, no. 1, pp. 122–131, 2009.